

## Chapter 3

# The Light Curve Morphology Analysis

This Chapter is focused on a study of the extremely close binary stars by the means of the Light Curve Morphology Analysis (LCMA). The LCMA constitutes of a set of methods I developed for studying the intrinsic variability of the lightcurves provided with the long time series photometry. My aim was to construct fast and reliable tools designed primarily to work with the data coming from large surveys, such as space borne photometry missions of Kepler, TESS or, in the near future, PLATO. The main motivation of this Chapter is to present the methods, as well as my findings on the long- and short-timescale activity in a sample of binaries I obtained with their help.

### 3.0.1 The first order light curve parameters

The basic principle of the LCMA is that it measures and describes the intrinsic variations of the light curve. I am defining the changes in the morphology (shape) of the lightcurve with the variation of parameters describing its extrema: the minima and the maxima of brightness. The great time resolution and mission span of the Kepler Space Telescope allows to study such variations in the subsequent orbital periods, even for object with an orbital period as short as several hours. The eight fundamental, *first order parameters* read from the lightcurve and used within the LCMA are:

- $h_{maxI}$  and  $h_{maxII}$  - the flux level at the primary and secondary maximum
- $h_{minI}$  and  $h_{minII}$  - the flux level at the primary and secondary minimum
- $\phi_{maxI}$  and  $\phi_{maxII}$  - the position of the primary and secondary maximum, expressed in the orbital phase ( $\phi$ )
- $\phi_{minI}$  and  $\phi_{minII}$  - the position of the primary and secondary minimum, expressed in the orbital phase

The LCMA in its purest form is limited to a model-independent description of the evolution of the above parameters in time (i.e. in the subsequent orbital periods). A well known example of a single parameter evolution is the O-C diagram, or a minima timing diagram. In fact, every diagram presenting an evolution of a given fundamental lightcurve parameter is a variant of the O-C diagram. For that reason I am departing from using this term. Instead, the diagrams presenting the variation of a given parameter in time will be referred to as the *evolutionary diagrams*.

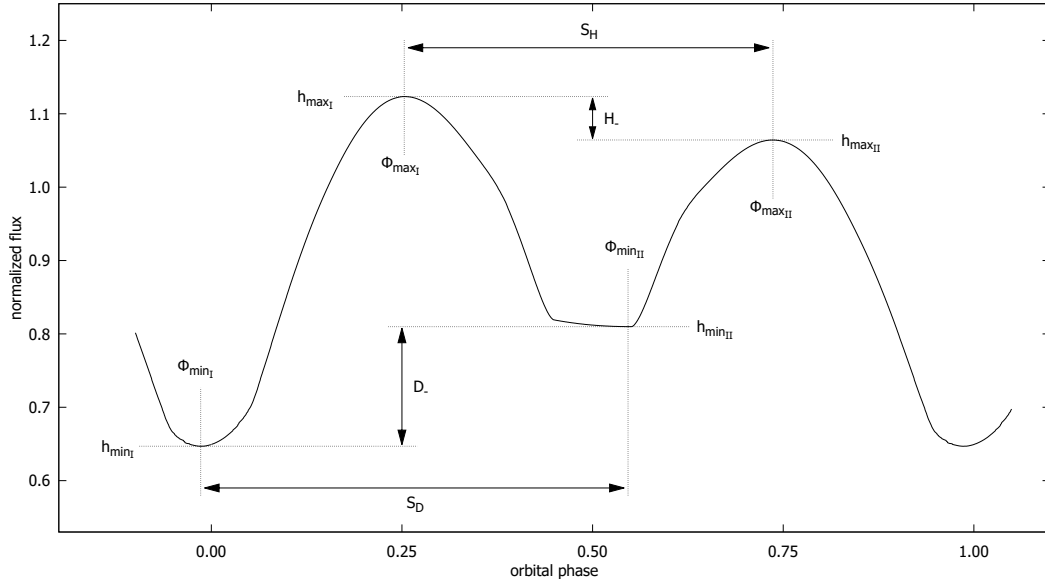


FIGURE 3.1: Parameters studied [...]

### 3.0.2 The second order light curve parameters

Further in this work I am showing the combinations of the fundamental parameters. A great example of such comes with the O'Connell effect, which essentially is the observation, that the brightness maxima of one phase curve are of unequal heights. I have toyed with all possible combinations of the first order parameters and selected six, which proved themselves most useful and interesting to present here. To unify the notation, I am introducing the following *second order light curve parameters*. These are: the difference ( $\mathbf{H}_-$ ) and the sum ( $\mathbf{H}_+$ ) of the brightness maxima levels, the difference ( $\mathbf{D}_-$ ) and the sum ( $\mathbf{D}_+$ ) of the brightness minima levels, the separation in orbital phase between the brightness maxima ( $\mathbf{S}_H$ ), and the separation in phase of the brightness minima ( $\mathbf{S}_D$ ). Specifically:

$$\begin{aligned}
 \mathbf{H}_+ &= h_{max_I} + h_{max_{II}} & [flux] \\
 \mathbf{H}_- &= h_{max_I} - h_{max_{II}} & [flux] \\
 \mathbf{D}_+ &= h_{min_I} + h_{min_{II}} & [flux] \\
 \mathbf{D}_- &= h_{min_I} - h_{min_{II}} & [flux] \\
 \mathbf{S}_H &= \phi_{max_{II}} - \phi_{max_I} & [\phi] \\
 \mathbf{S}_D &= \phi_{min_{II}} - \phi_{min_I} & [\phi]
 \end{aligned} \tag{3.1}$$

Following the above definitions, the  $\mathbf{H}_-$  is the measure of the O'Connell effect. Its analog for the minima is the  $\mathbf{D}_-$ . Please refer to Fig. 3.1 for the graphical presentation of the newly introduced parameters. The data here are taken primarily from the Kepler Eclipsing Binary Catalogue<sup>1</sup> (KEBC, Slawson et al., 2011), which provides light curves normalized to the mean flux level across an entire observational span. I decided to remain within the realm of flux instead of switching to magnitudes, but the LCMA can be easily adopted to magnitudes with some trivial transformations.

<sup>1</sup><http://keplerebs.villanova.edu>, accessed June 2016

### 3.0.3 The observational data

As already mentioned, the great majority of the observational data presented here come from the KEBC. The LCMA was originally intended to be used for contact binaries only, but it quickly turned out to be easily applicable to a more general set of objects. To do so, they have to follow a simple rule - to exhibit brightness both minima and maxima - i.e. to have the EW- or EB-type light curves, or as the 'ellipsoidal' ones (presumably non-eclipsing close binaries with a prominent tidal distortions). For that reason I am distinguishing three data sets originating from the Kepler mission:

- The `FB-Sample`, most important, most widely used in this work. It consists of 48 objects from KEBC with the EW-type light curves with the minima of similar depths and orbital period  $P < 1$  d, each inspected individually by eye. All objects in this sample experience a total eclipse event (flagged as flat-bottom, FB, in KEBC). I have performed a quick modeling of a mean light curve for every object in this sample to confirm its contact binary nature. I am using the `FB-Sample` to be sure that the primary minimum occurs during the transit of the less massive component in front of the more massive primary. This will be most important in Section 3.1. The `FB-Sample` has a unique trait: all its members have very similar inclination, close to  $90^\circ$ .
- The `EW-Sample` consists of 426 contact binary candidates I have selected from KEBC. It consists of objects with light curves of the EW-type selected by eye. This subset largely coincides with the list of objects identified as 'overcontact binaries' in KEBC Version v0.96 (Prša et al., 2011). The `FB-Sample` is fully enclosed within the `EW-Sample`. The main purpose for this sample is to show the results of the use of the LCMA on objects with a generally unknown morphology, but with the EW-type light curve. In other words, I am using the `EW-Sample` as a generalization of my findings made during the analysis of the `FB-Sample` (e.g. during the analysis of the interchanging minima depths in Section 3.2 or in the statistical study of the light curve activity in Section 3.7).
- The `ALL-Sample`, the widest sample from KEBC. It consists of 1216 objects selected by just one criterion: to have parameter  $morph > 0.6$ . This is a rule of thumb to select the objects with light curves of 'at least' EB-type. For more details on the parameter please refer to Slawson et al. (2011). These objects were not preselected by eye, and no physical, nor geometrical assumptions are made for them. This set is used for the most general statistical studies at the end of this Chapter.

Additionally, in Section 3.1 I am introducing the multicolor data taken with the ground-based telescopes. These objects are gathered into a fourth, separate sample.

- The `SUH-Sample` consists of 38 objects taken from the Mt. Suhora' Observatory website<sup>2</sup>. These are confirmed contact binaries observed in *UBVRI* Bessel photometric system. All objects in the `SUH-Sample` have their mass ratio determined spectroscopically. The use of this sample, as well as its analysis is strictly limited to Section 3.1. The detailed description of these particular data is included in Section 3.1.2.

<sup>2</sup>[www.as.up.krakow.pl](http://www.as.up.krakow.pl), accessed in October 2017

### 3.0.4 The LCMA and the stellar magnetic activity

The full, model dependent, extension of the LCMA takes into account the theoretical background of the intrinsic light curve variations. The main paradigm of the Analysis presented in this work is that the intrinsic variations are caused by the photospheric phenomena on the surface of the binary. For the simplicity such photospheric phenomena will be called here 'starspots' or 'spots' with no intention of implying their physical origin. Obviously, the starspots presented in Chapter 1 were inclined to be caused by the magnetic activity and that presumption will be taken into account later, during the discussion and interpretation of the the results in Chapter 4. A starspot here, as understood in LCMA, is simply a region of a photosphere with a different effective temperature (hence different brightness) than their surrounding stellar surface. In order to analyze and understand the evolutionary diagrams of the observational data I have simulated a large set of synthetic light curves of contact binaries experiencing a longitudinal starspot migration. To limit the number of the introduced parameters, the simulated spot is circular and described by four parameters only: its radius ( $r_{spot}$  [°]), the co-latitude and longitude of its center ( $\lambda$  and  $\varphi$  respectively, [°]) and its temperature (regarded as a fraction of the effective temperature of its host star,  $T_x$ , where  $x$  is 1 for the primary component or 2 for the secondary).

The numerical simulations were performed with three separate grids. Two of them concerned the light curves of systems experiencing a spot migration, while the third one focused only on the parameter  $S_H$ , the separation of the maxima, in systems with no spot-related activity. All synthetic light curves were simulated with the Wilson-Devinney code (2013 version<sup>3</sup>) modified slightly to automate the process. The synthetic light curves in every grid were simulated with a narrow step in the orbital phase,  $\Delta\phi = 0.00001$ , the square root limb darkening law has been used, the gravitational brightening coefficient was set to  $\beta = 0.08$ , and the W-D code operated in MODE=3. A brief description of the grids is given below.

- The MigraGrid was created to study the evolutionary signals of light curve extrema produced by migrating starspots. The grid covers a wide range of contact binaries varying in inclination, mass ratio and fill-out factors with a variety of starspot types (sizes and locations) moving longitudinally. The simulations assume that the circular starspot completes one full cycle of the migration and that there is only one of such on a surface of a binary at the time. By the 'cycle of migration' I understand one full migration, i.e.  $360^\circ$  along the stellar longitude, of a starspot at a fixed co-latitude. During the migration cycle the spot do not change its temperature, nor its size. In this grid all simulations are performed for the Kepler mission photometric filter,  $K_p$ . The binaries in the MigraGrid have components of an equal effective temperature:  $T_1 = T_2 = 6000$  K, the spots have a fixed temperature of  $T_{spot} = 0.8 T_1$ , and migration step is chosen as  $\Delta\phi = 10^\circ$ . I have used this grid to test most general ideas on how the profiles of the evolutionary signals should look like for different spots in different light curve parameters. The details on parameters space in the MigraGrid are gathered in Tab. 3.1.
- The DenseGrid has been prepared to study the evolutionary signals with a better precision and to provide better visual materials. In this grid I am using only one model of a contact binary. The parameters of the underlying contact

<sup>3</sup><ftp://ftp.astro.ufl.edu/pub/wilson/lcdc2013/>, accessed October 2016

binary are based on the results from the numerical modeling of KIC 6118779. Although the system parameters are fixed, the parameters of the migrating spot are sampled with a smaller step,  $\Delta\phi = 1^\circ$ . The remaining details on the parameter space in DenseGrid are shown in Tab. 3.2. Please note that the light curves for the cases of a migration of the special kind of starspots (e.g. starspot on a secondary or a hot spot) are build on the same model system as the DenseGrid is.

- The SepaGrid is the only one not concerning the starspot migration. It is also the only grid presented here with the simulation made additionally for the wide band photometric Bessel filters *UBVRI*. SepaGrid was designed to deal with the problem of a possible connection between the separation of the brightness maxima and the mass ratio of the system. This issue will be addressed in Section 3.1. The parameters describing the third grid are in Tab. 3.3.

### 3.0.5 PerSiL - the automatization of the LCMA

To automatize the process of data preparation and initial analysis I have prepared a computer program, code name PerSiL (**P**eriodic **S**ignals in **L**ight curves). The program is divided into two distinctive modules: one for the preparation and analysis of the observational data and second is to handle the numerical modeling. PerSiL is written primarily as a bash script and consists of several peripheral programs I wrote or adopted to my needs (in C and FORTRAN languages). The core of the numerical simulations module of PerSiL is based on the LC part of the Wilson-Devinney code. The User can simulate a set of synthetic light curves with one or several parameters changing by a set step. The light curves can be simulated in the orbital phase range set by User. For example, when constructing the SepaGrid I simulated only the orbital phases near the primary and secondary maxima (0.15-0.35  $\phi$  and 0.65-0.85  $\phi$ , accordingly) to save the computational time.

The observational data treatment module of PerSiL has its own user interface and configure file. Having provided the list of objects along with some basic information about their light curves, PerSiL downloads their data from the KEBC, and rephases the light curves. Alternatively, it operates on the light curves provided by the user. Then, PerSiL automatically determines the fundamental light curve parameters (the  $h_{maxI}$ ,  $h_{minI}$  etc.) in subsequent orbital periods. In the next step, PerSiL performs the light curve folding. The exposure time of Kepler's Long Cadence of 0.5 hour yields less than 20 data points per orbital phase of a typical contact binary. That in turn results in the undersampled lightcurves around the extrema. (Rucinski, 2015) and (Slawson et al., 2011) chose to search for the minima timing in such undersampled light curves and then perform a running average on the results. I am approaching the issue the other way around: I am folding the light curves prior the minima/maxima search. The rule of thumb was that one folded phase curve (i.e. complete light curve covering orbital phases from 0.0 to 1.0) should have no less that 120 datapoints. Having significantly less data points per phase curve could end with the algorithm for the determination of the parameters of the given extreme fail or return a highly dubious results. On the other hand, I found that some light curves evolved so rapidly, that folding more than eight orbital epochs could end in a removal of the valuable information by smoothing of the evolution signals too much (eg. KIC 5809868 or KIC 6067735). The 120 data point threshold seemed like a good trade-off. PerSiL is establishing how many orbital periods should be folded together

TABLE 3.1: The boundaries of the parameters in the MigraGrid.

system parameters			
parameter	lower boundary	upper boundary	step
$i$ [ $^{\circ}$ ]	50	90	5
$ff$	0.0	1.0	0.1
$q$ [ $M_2/M_1$ ]	0.1	1.0	0.1
spot parameters			
parameter	lower boundary	upper boundary	step
$r_{spot}$ [ $^{\circ}$ ]	10	50	10
$T_{spot}$ [ $T_1$ ]	0.80	(fixed)	
$\lambda$ [ $^{\circ}$ ]	0	90	10
$\varphi$ [ $^{\circ}$ ]	0	359	10

TABLE 3.2: The boundaries of the parameters in the DenseGrid.

spot parameters			
parameter	lower boundary	upper boundary	step
$r_{spot}$ [ $^{\circ}$ ]	5	60	5
$T_{spot}$ [ $T_1$ ]	0.4	0.9	0.1
$\lambda$ [ $^{\circ}$ ]	0	170	5
$\varphi$ [ $^{\circ}$ ]	0	359	1

TABLE 3.3: The boundaries of the parameters in the SepaGrid.

parameter	lower boundary	upper boundary	step
$i$ [ $^{\circ}$ ]	20	70	5
	70	90	2
$ff$	0.0	1.0	0.1
$q$ [ $\frac{M_2}{M_1}$ ]	0.1	1.0	0.1
$T_1$ [K]	4000	7000	1000
$T_2$ [K]	4000	7000	1000

for each studied system (for example, it is 9 epochs for an object with the orbital period of 0.3 days). Then, the box-car folding-function is being moved every orbital period. For that reason one must be very careful when analyzing the structures in the evolutionary diagrams which are of extremely short periodicity (several epochs). I have chose this method to study the possible short-living or abrupt events in the light curve evolution, some of which needed the resolution of only two or three orbital epochs (e.g. KIC 8145477 or KIC 8804824).

The use of the Short Cadence (SC) Kepler observations (sampled every minute) would be restricted to just two objects with the EW-type light curve and a flat-bottom-profiled secondary minimum. Moreover, such data cover a shorter time

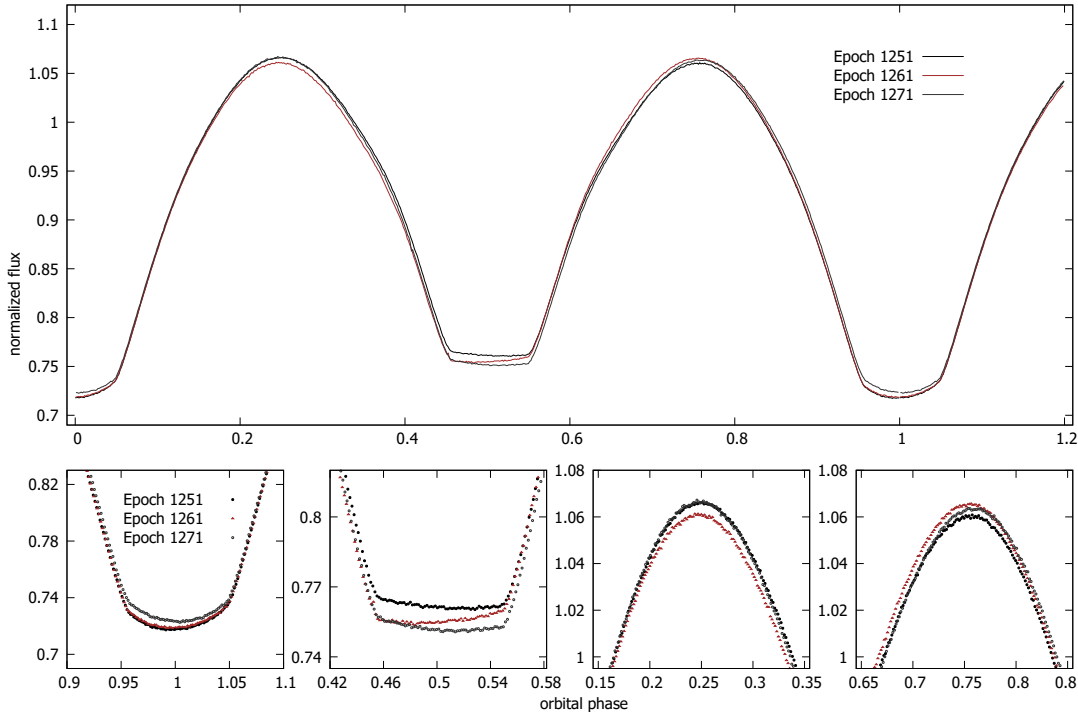


FIGURE 3.2: Fine changes in the light curve of a contact binary KIC 8496820. The lightcurves come from the Short Cadence mode of the Kepler Spacecraft.

span, typically of about one month. Such data would be very unfortunate for a comprehensive study. It must be noted here, that although there is not enough SC data for a proper analysis, it may serve as a great example of some fine effects of the light curve intrinsic variability. In Fig. 3.2 I am showing such phenomena in the light curve of a contact binary KIC 8496820. The three phase curves in the upper panel are exhibiting different distortions, which can be studied in detail in the four bottom panels. I have gathered there the profiles of the extrema (starting from left): the primary and the secondary minimum and the primary and the secondary maximum. Please note how the secondary minimum varies and that its depth changes hardly coincides with the changes of its tilt. The phase curves presented in the Figure are separated by 10 orbital epochs only. It means that such small but significant light curve evolution occur on a time scale of just three days.

In the next step, PerSiL is performing the search of the extrema using several approaches, two of which are used in this work. First, which I called the *precise determination*, is a 7-th order polynomial fit to the appropriate range of phase curve ( $0.15\phi - 0.35\phi$  and  $0.65\phi - 0.85\phi$  in search of the maxima and  $0.4\phi - 0.6\phi$  and  $0.9\phi - 1.1\phi$  for the parameters of the minima). This method aims at establishing a true moment and phase of the brightness minimum or maximum. This data are going to be utilized during the analysis of the light curve distortions. The use of such a high order polynomial as a fitting function was grounded by my previous work I described in my Master Thesis (Debski, 2012). The second approach in the search of the extrema incorporated a simple parabola fit to the same ranges as in the previous method. This approach was introduced for maintaining the consistency with the measurements from the literature (e.g. Rucinski, 2015; Slawson et al., 2011). The discussion on the two approaches is developed further in Section 3.2.2.

After the determination of the fundamental light curve parameters, PerSiL stores

the results in a separate output file. The parameters are tied to their central epochs, around which the light curve has been folded. The temporary files containing the folded light curves for every single central epoch are also saved, along with their plotted versions (saved as PNG files), if the user chooses so. In the next step, PerSiL computes the second order light curve parameters out of those stored in the output file and removes outlying datapoints. The cleaning mechanism is a running function of a fixed width and the step of one epoch. The clipping is set by default to two sigma as the best result result of the trial and error method. Later, such prepared evolutionary diagrams of the second order light curve parameters are subjected to the basic statistics. PerSiL stores the information about the median and arithmetical mean of each second order parameter, as well as their interquartile range and standard deviation. Some examples of the output data and images are presented in the appendixes to this work. All catalogue of ALL-Sample objects with their output produced with PerSiL is accessible via my web page<sup>4</sup> or upon request.

Before we dive into the analysis of the light curve evolution, we need a firm method for determination, which minimum is the primary one. To recapitulate, during the primary minimum, if the system is an eclipsing binary, the less massive star (secondary component) is transiting in front of the more massive, primary component. The masses of the primary and secondary components are:  $M_1$  and  $M_2$ . In case of non-eclipsing binaries, in which the minima are caused by the ellipsoidal effect, the definition is analogous but with a lowered inclination taken into account. This issue becomes very complicated for binaries with components of a similar surface temperatures and no total eclipse events. The best example of such systems are contact binaries of W UMa type, in which both components share a common convective envelope. The (nearly) equal depth of the minima as well as the known interchange of their depth in time in some cases (with examples known as early as, for instance, Binnendijk, 1960, and discussed in deep in Section 3.2.2) makes it extremely troublesome to establish a 'proper' primary minimum. Of course, one could conduct a numerical modeling of every light curve twice, with a half orbital phase shift in each modeling run other and see, which result fit the data better. For the rather obvious reasons, this approach would be highly ineffective. We should employ, if possible, another straightforward, intrinsic characteristic of a light curve for this task. Since we cannot rely on the brightness minima, an alternative method is needed.

---

<sup>4</sup><http://www.ou.uj.edu.pl/B.Debski/>